Proton Beam Radiotherapy - The State of the Art[1]

Harald Paganetti and Thomas Bortfeld

Massachusetts General Hospital, Boston, MA, USA

1. Introduction

a - Physical Rationale

Protons have different dosimetric characteristics than photons used in conventional radiation therapy. After a short build-up region, conventional radiation shows an exponentially decreasing energy deposition with increasing depth in tissue. In contrast, protons show an increasing energy deposition with penetration distance leading to a maximum (the "Bragg peak") near the end of range of the proton beam (figure 1).

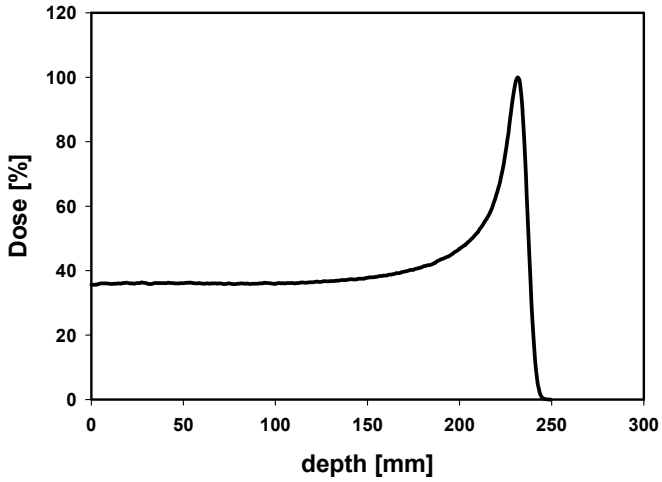

Figure 1: Typical dose deposition as a function of depth for a proton beam.

Protons moving through tissue slow down loosing energy in atomic or nuclear interaction events. This reduces the energy of the protons, which in turn causes increased interaction with orbiting electrons. Maximum interaction with electrons occurs at the end of range causing maximum energy release within the targeted area. This physical characteristic of protons causes an advantage of proton treatment over conventional radiation because the region of maximum energy deposition can be

[1] To be published in: New Technologies in Radiation Oncology (Medical Radiology Series)
(Eds.) W. Schlegel, T. Bortfeld and A.-L. Grosu
Springer Verlag, Heidelberg, ISBN 3-540-00321-5, October 2005

positioned within the target for each beam direction. This creates a highly conformal high dose region, e.g., created by a spread-out Bragg peak (SOBP) (see section 3a), with the possibility of covering the tumor volume with high accuracy. At the same time this technique delivers lower doses to healthy tissue than conventional photon or electron techniques. However, in addition to the difference in the depth-dose distribution there is a slight difference when considering the lateral penumbra (lateral distance from the 80% dose to the 20% dose level). For large depths the penumbra for proton beams is slightly wider than the one for photon beams by typically a few mm.

b - Clinical Rationale

The rationale for the clinical use of proton beams is the feasibility of delivering higher doses to the tumor, leading to an increased tumor control probability (TCP) (Niemierko et al., 1992). This is possible due to the irradiation of a smaller volume of normal tissues compared to other modalities. Due to the reduced treatment volume and a lower integral dose, patient tolerance is increased. Like other highly conformal therapy techniques, proton therapy is of particular interest for those tumors located close to serially organized tissues where a small local overdose can cause fatal complication such as most tumors close to the spinal cord. Irregular shaped lesions near critical structures are well suited for protons.

Proton therapy has been applied for the treatment of various disease sites (Delaney et al., 2003) including paranasal sinus tumors (Thornton et al., 1998), chordoma (Benk et al., 1995; Terahara et al., 1999), chondrosarcoma (Rosenberg et al., 1999), meningioma (Hug et al., 2000; Wenkel et al., 2000), prostate (Hara et al., 2004; Slater et al., 2004), and lung tumors (Shioyama et al., 2003). Clinical gains with protons have long been realized in the treatment of uveal melanomas, sarcomas of the base of skull (Weber et al., 2004), and sarcomas of the paravertebral region. Proton radiosurgery has been used to treat large arterial venous malformations as well as other intracranial lesions (Harsh et al., 1999).

Treatment plan comparisons show that protons offer potential gains for many sites. Comparisons of treatment modalities (protons vs. photons) have been made on the basis of TCP and NCTP (Normal Tissue Complication Probability) calculations for

cranial irradiation of childhood optic nerve gliomas by Fuss et al. (Fuss et al., 2000). Also, advantages of proton plans compared to photon plans have been shown for pediatric optic pathway gliomas (Fuss et al., 1999) and for pediatric meduloblastoma / primitive neuro-ectodermal tumors (Miralbell et al., 1997). Here, proton therapy offered a high degree of conformity to the target volumes and steep dose gradients, thus leading to substantial normal tissue sparing in high- and low-dose areas. Studies on various CNS tumors and pediatric patients with low-grade astrocytoma revealed that acute or early late side effects were low (McAllister et al., 1997; Hug and Slater, 1999). Another target used for comparative treatment planning is glioblastoma multiforme (Tatsuzaki et al., 1992) where, due to a highly radioresistant tumor mass and due to extensive microscopic invasion, high doses to critical structures are difficult to avoid. A comparison of proton and X-ray treatment planning for prostate cancer has been published by Lee et al. (Lee et al., 1994). Others studied X-ray and proton irradiation of esophageal cancer (Isacsson et al., 1998), locally advanced rectal cancer (Isacsson et al., 1996), and paraspinal tumors (Isacsson et al., 1997) showing that protons have therapeutic advantages over conventional therapy based on TCP and NTCP calculations. Osteo- and chondrogenic tumors of the axial skeleton, rare tumors at high risk for local failure, were studied for combined proton and photon radiation therapy (Hug et al., 1995). The potential advahintages of protons has also been discussed for various other types of tumors (Archambeau et al., 1992; Levin, 1992; Miralbell et al., 1992; Nowakowski et al., 1992; Slater et al., 1992; Slater et al., 1992; Smit, 1992; Tatsuzaki et al., 1992; Tatsuzaki et al., 1992; Wambersie et al., 1992; Lee et al., 1994; Lin et al., 2000).

For advanced head and neck tumors a treatment plan comparison was done by Cozzi et al. (Cozzi et al., 2001) for five patients using 3D conformal and intensity modulated photon therapy and proton therapy. They distinguished between passive and active modulated proton beams (see section on Proton Beam Delivery). They concluded that looking at target coverage and tumor control probability there are only small differences between highly sophisticated techniques like protons or intensity modulated photons if the comparison is made against good conformal treatment modalities with conventional photon beams. The situation was judged to be quite different if organs at risk were considered.

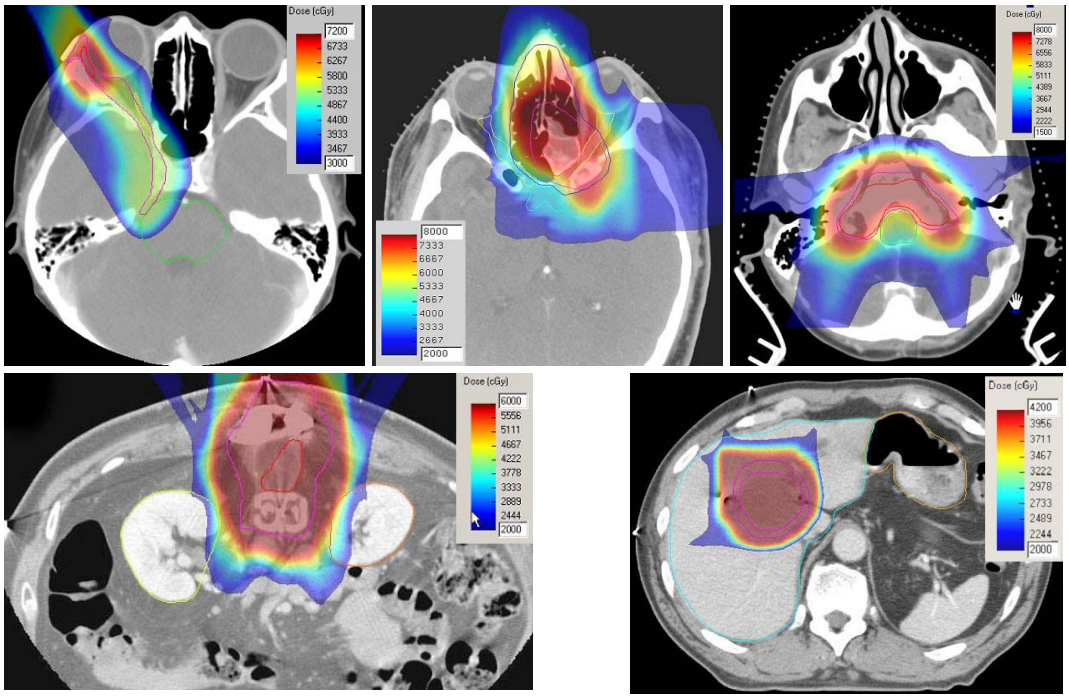

Figure 2: Proton dose distributions with dose displays in Cobalt Gray Equivalent (CGE): Upper row (left to right): Adenocyctic carcinoma of the lacrimal gland prescribed to a CTV and GTV dose of 56 and 72 CGE respectively, minimizing the irradiation of the nearby temporal lobes; Paranasal sinus tumor prescribed to a CTV and GTV dose of 54 and 76 CGE respectively, minimizing the dose to the temporal lobes, brainstem, orbits, optic nerves and chiasm; Skull base chordoma prescribed to a CTV and GTV dose of 50 and 80 CGE respectively, avoiding the brainstem. Lower row: Lumbar spine chordoma prescribed to 60 CGE avoiding the kidneys and small bowel; Hepatoma prescribed to 42 CGE minimizing the dose to the normal portion of the liver. (Bussiere and Adams, 2003)

A treatment plan comparison for conventional proton, scanned proton, and intensity modulated photon radiotherapy, was performed by Lomax et al. (Lomax et al., 1999) using CT scans and planning information for nine patients with varying indications and lesion sites. The results were analyzed using a variety of dose and volume based parameters. They found that the use of protons could lead to a reduction of the integral dose by a factor of three compared to standard photon techniques and a factor of two compared to intensity modulated photon plans. Further, optimized

treatment plans for intensity modulated X-ray therapy (IMXT), VEEHT (very high energy electron therapy), and intensity modulated proton therapy (IMPT) were compared for prostate cancer (Yeboah and Sandison, 2002). It was concluded that IMPT delivered a mean rectal dose and a bladder dose that was much lower than achievable with the other two modalities. IMPT was also superior in target coverage. Figure 2 demonstrates the conformality achievable with conventional proton therapy for various body sites.

Due to the reduction in integral dose with protons, the most important benefits can be expected for pediatric patients. In this group of patients there is much to be gained in sparing normal tissue that is still in the development stages. Examples are treatments of retinoblastoma, meduloblastoma, rhabdomyosarcoma and Ewing's sarcoma. In the treatment of retinoblastoma one attempts to limit the dose to the bone, adjacent brain, contra-lateral eye and the affected eye's anterior chamber. In the treatment of meduloblastoma the central nervous system including the whole brain and spinal canal are irradiated while sparing the cochlea, pituitary gland and hypothalamus. The benefits of protons are obvious when considering the reduced heart, lung and abdominal doses compared with X-rays. A typical meduloblastoma dose distribution is shown in figure 3 (Bussiere and Adams, 2003).

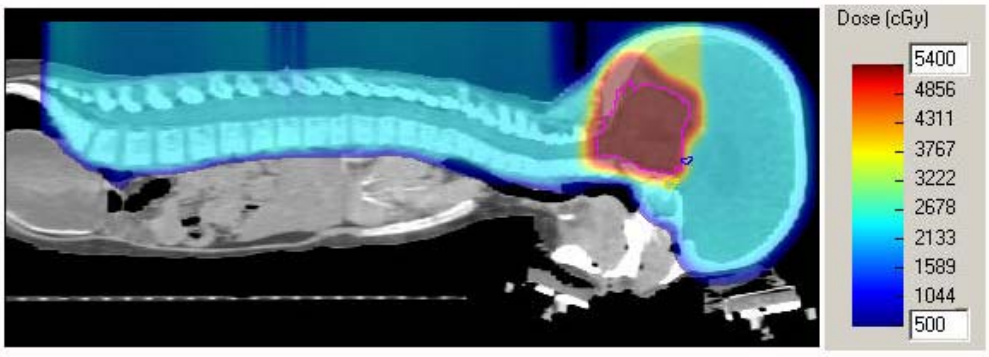

Figure 3: Sagital color-wash dose display for the treatment of meduloblastoma including the CSI to 23.4 CGE as well as the posterior fossa boost to 54 CGE. (Bussiere and Adams, 2003)

It is evident from photon/proton comparisons that even with the rapid development of intensity-modulated dose delivery with electrons and photons, protons are capable of much higher dose conformity, in particular for intensity modulated proton

techniques (Lomax et al., 1999; Lomax et al., 2003; Lomax et al., 2003; Weber et al., 2004). The reduction of integral dose with protons is also significant. Although it is true that the clinical relevance of low doses to large volumes is not well known (except perhaps in organs with a parallel or near parallel architecture), there are cases where a reduction in overall normal tissue dose is proven to be relevant, e.g., for pediatric patients (Lin et al., 2000).

c – Worldwide proton therapy experience

Institution	**Where**	**First Treatm.**	**Last Treatm.**	**Number of Patients**	**Date of total**
Berkeley 184	CA, USA	1954	1957	30	
Uppsala	Sweden	1957	1976	73	
Harvard	MA, USA	1961	2002	9116	
Dubna	Russia	1967	1996	124	
ITEP, Moscow	Russia	1969		3748	June-04
St. Petersburg	Russia	1975		1145	April-04
Chiba	Japan	1979		145	Apr-02
PMRC[1], Tsukuba	Japan	1983	2000	700	
PSI (72 MeV)	Switzerland	1984		4066	June-04
Dubna	Russia	1999		191	Nov-03
Uppsala	Sweden	1989		418	Jan-04
Clatterbridge	England	1989		1287	Dec-03
Loma Linda	CA, USA	1990		9282	July-04
Louvain-la-Neuve	Belgium	1991	1993	21	
Nice	France	1991		2555	April-04
Orsay	France	1991		2805	Dec-03
iThemba LABS	South Africa	1993		446	Dec-03
MPRI[1]	IN, USA	1993	1999	34	
UCSF - CNL	CA, USA	1994		632	June-04
TRIUMF	Canada	1995		89	Dec-03
PSI (200 MeV)	Switzerland	1996		166	Dec-03
H. M. I, Berlin	Germany	1998		437	Dec-03
NCC, Kashiwa	Japan	1998		270	June-04
HIBMC, Hyogo	Japan	2001		359	June-04
PMRC[2], Tsukuba	Japan	2001		492	July 04
NPTC, MGH	MA, USA	2001		800	July-04
INFN-LNS,Catania	Italy	2002		77	June-04
WERC	Japan	2002		14	Dec-03
Shizuoka	Japan	2003		69	July-04
MPRI[2]	IN, USA	2004		21	July -04
			Total	39612	

Table 1: World wide proton therapy experience as of July 2004. (Sisterson, 2004)

Robert Wilson first proposed the use of protons for radiation therapy at Harvard in 1946 (Wilson, 1946). The first patient was treated in 1954 at Lawrence Berkeley Laboratory (Tobias et al., 1958). About 40,000 patients have received proton therapy to date worldwide (see Table 1) (Sisterson, 2004).

Although the number of patients being treated with protons is steadily increasing, as are the number of facilities operating worldwide, it is still only a small fraction of radiotherapy patients overall that are treated with protons. One reason for this is the cost of a proton facility. Sophisticated proton therapy is now, and is likely to continue to be, more expensive than sophisticated (i.e., intensity-modulated) X-ray therapy. The construction cost of a current two-gantry proton facility, complete with the equipment, was estimated to be about 4 times the cost of a two-linac X-ray facility (Goitein and Jermann, 2003). According to Goitein and Jermann (Goitein and Jermann, 2003) the cost of operation of a proton therapy facility is dominated by the business cost (42%, primarily the cost of repaying the presumed loan for facility construction), personnel costs (28%) and the cost of servicing the equipment (21%). For X-ray therapy, the cost of operation was estimated to be dominated by the personnel cost (51%) and the business costs (28%). The ratio of costs of proton vs. X-ray therapy per treatment fraction is about 2.4 at present.

2. Proton Accelerators

a - Cyclotron

A cyclotron consists of dipole magnets designed to produce a region of uniform magnetic field. These dipoles are placed with their straight sides parallel but slightly separated. An electric field is produced across the gap by an oscillating voltage. Particles injected into the magnetic field region move on a semicircular path until they reach the gap where they are accelerated. Since the particles gain energy they will follow a semi-circular path with larger radius before they reach the gap again. In the meantime the direction of the field has reversed and so the particles are accelerated again. As they spiral around particles gain energy. Thus, they trace a larger arc with the consequence that it always takes the same time to reach the gap.

The size of the magnets and the strength of the magnetic fields limits the particle energy that can be reached by a cyclotron.

The first cyclotrons being used for proton therapy were initially designed for physics research and were later turned into treatment facilities. Currently more and more cyclotrons are specifically built and dedicated for use in radiation therapy. The envisaged targets in the human body define the specifications for such a cyclotron. The maximum proton beam energy is directly related to the maximum depth in tissue. Low-energy proton beams can only be used for superficial tumors. For example, many cyclotrons currently being used in proton therapy have an energy limit around 70 MeV, which suits them only for treating ocular tumors. In order to be able to treat all common tumors in the human body, the cyclotron has to be able to deliver a beam with energy of up to about 230 MeV, which corresponds to a range in tissue of about 32 cm. However, one has to consider that the maximum penetration of the proton beam in the patient is reduced if the beam has to be widened by absorbers to reach large field sizes. Field sizes of up to 30 x 30 cm^2 may be required. While being able to deliver energies that can be used to cover common tumor sizes and locations the cyclotron has to deliver a dose rate acceptable for treatment, i.e. at least around 2 Gy/min. With respect to the dose rate one has to keep in mind that the efficiency of a beam delivery system is never 100%. In particular for double-scattering systems (see section 3a) it can be as low as 20%. Cyclotron intensities can exceed hundred mA but they can be hardware limited at the ion source to several hundreds of nA, which corresponds to clinically meaningful dose rates. Higher currents are not safe for treatment because of the small feedback time for machine control. Cyclotrons that are used in a purely clinical environment require a high grade of reliability, low maintenance and should be easy to operate. In fractionated radiation therapy, machine downtimes should be minimized because this may result in the necessity to re-calculate daily doses because of tissue repair effects.

Cyclotrons can be either isochronous or synchrocyclotrons. In addition, they can be superconducting. In an isochronous cyclotron the orbital period is the same for all particles regardless of their energy or radius. Thus, the RF power can operate at a single frequency. Isochronous cyclotrons provide a continuous beam. Since the acceleration of particles in a cyclotron takes usually only tenths of a ms, the beam

(i.e. via an external injection system) can be turned on and off very quickly. This is an important safety feature. It also allows the beam current to be modified during delivery with very short response times. Both these features are very important when it come to proton beam scanning techniques for patient treatment (see section 3b). Superconducting cyclotrons have advantages compared to non-superconducting ones in that they are smaller and not as heavy (Blosser et al., 1989).

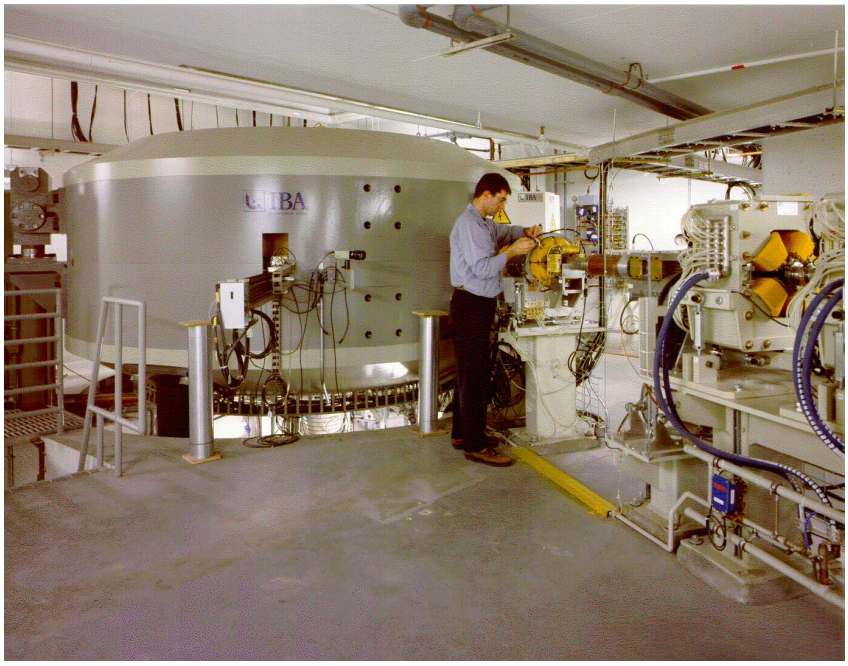

Figure 4 Isochronous cyclotron by Ion beam Applications, S.A. It extracts protons with an energy of 230 MeV, which corresponds to a range of a ~33.0 cm in Water. Picture provided by Ion Beam Applications, S.A.

Figure 4 shows a typical example of a cyclotron dedicated for use in radiation therapy. The magnetic field is generated by 4 sectors with an external yoke diameter of 4.3 m. The system weighs about 200 tons.

Since the cyclotron is extracting particles with a fixed energy, an energy selection system is needed in the beamline (figure 5). The energy selection system consists of a degrader of variable thickness to intercept the proton beam, i.e. a carbon wedge that can be moved in and out of the beam quickly. As a result of the energy degradation, there is an increase in emittance and energy spread, which can be controlled by slits and magnets. The emittance can be defined as the sum of the

phase space areas (or by the area, which encloses the phase space). The phase space of a beam is the distribution of particle position versus momentum direction.

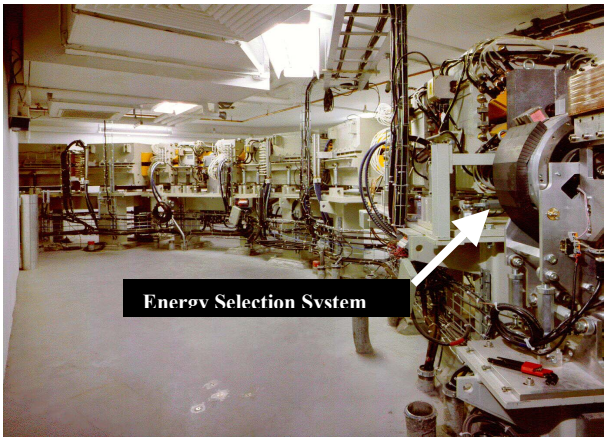

Figure 5: Part of the beamline at the Northeast Proton Therapy Center including the energy selection system to modulate the fixed energy extracted from the cyclotron. Picture provided by Ion Beam Applications, S.A.

b - Synchrotron

A synchrotron is a circular accelerator ring. Electromagnetic resonant cavities around the ring accelerate particles during each circulation. Since particles move always on the same radius, the strength of the magnetic field that is used to steer them must be changed with each turn because the particles energy increases. Because of this synchronization of field strength and energy, these accelerators are called synchrotrons. This technique allows the production of proton beams with a variety of energies (unlike the cyclotron which has a fixed extraction energy). A small linear accelerator is often used to pre-accelerate particles before they enter the ring.

One disadvantage of cyclotrons is the inability to change the energy of the extracted particles directly. Energy degradation by material in the beam path leads to an increase in energy spread and beam emittance and reduces the efficiency of the system. Another consequence is the need for more shielding because it leads to secondary radiation. In this respect a synchrotron is a more flexible solution. A synchrotron allows beam extraction for any energy. Synchrotrons are, however, much bigger than cyclotrons. A synchrotron delivers a pulsed beam, i.e. it accelerates and extracts protons with a specific repetition rate. Fast extraction

delivers the beam after a single turn. This avoids complicated feedback systems. However, for therapeutic applications, slow extraction is needed for machine control reasons. Here the typical extraction pulse is a few seconds. Table 2 compares different proton therapy accelerator technologies (Coutrakon et al., 1999).

Type	Synchrotron (rapid cyle)	Synchrotron (slow cyle)	Cyclotron
Energy level selection	Continuous	Continuous	Fixed
Size (diameter) [m]	10	6	4
Average power (beam on)[kW]	200	370	300
Emittance (RMS unnorm.) [µm]	0.2	1-3	10
Repetition rate [Hz]	60	0.5	Continuous
Duty factor (beam-on time)	Pulses	20%	Continuous

Table 2: Accelerator technology comparisons for some parameters (Coutrakon et al., 1999).

c - Beam Line

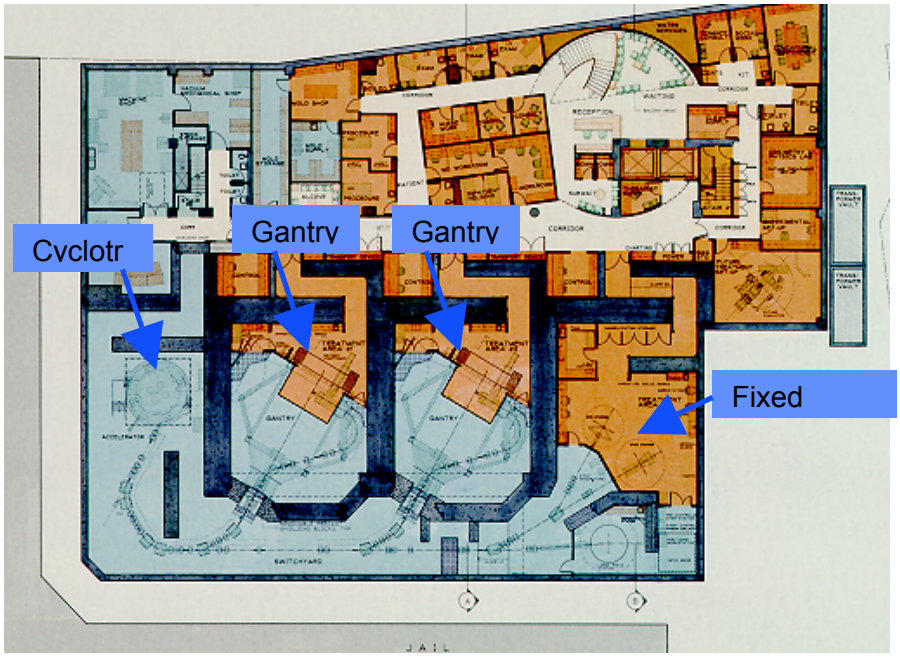

Figure 6: Floor plan of the Northeast Proton Therapy Center. Drawing provided by Ion Beam Applications, S.A.

The beam has to be transported from the cyclotron to the treatment room(s) using magnets for bending, steering and focusing. In addition, as a safety precaution, detectors monitoring the beam's phase space are located in the beamline. These devices control certain tolerances for beam delivery. Figure 5 shows part of the beamline that transports the beam from the cyclotron to different treatment rooms at the Northeast Proton Therapy Center (NPTC). Figure 6 shows a typical floor plan of a treatment facility (Flanz et al., 1995).

Table 3 lists the clinical performance specifications of the NPTC (Flanz et al., 1995), which is based on an isochronous cyclotron and two gantry treatment rooms with double scattering systems as well as one treatment room with horizontal beamlines. These parameters are defined to ensure safe dose delivery taking into account the precise dose deposition characteristics of protons.

d - Gantry/Fixed Beams

With a fixed horizontal beamline patients can usually be treated only in a seated or near-seated position. However, conformal radiation therapy usually requires multiple beams coming in from different directions. In order to irradiate a patient from any desired angle the treatment head has to be able to rotate. This makes it much easier to position the patient in a reproducible way and similar to the way the patient was positioned during imaging prior to planning and treatment. The ability to deliver beams from various directions is achieved by a gantry system (figure 7). The beam has to be deflected by magnetic fields in the gantry. Gantries are usually large structures because, firstly protons with therapeutic energies can only be bent with large radii, and secondly beam monitoring and beam shaping devices have to be positioned inside the treatment head affecting the size of the nozzle. The nozzle at the NPTC has a length of about 2.5 m, which results in a distance between isocenter and beam entering the gantry of about 3 m. Eccentric gantries are used to reduce the size (Pedroni et al., 1995). To ensure precise dose delivery the mechanics of the gantry has to be able to keep the isocenter of rotation always within 1 mm under all rotation angles. This requires careful design of the mechanical structure since the overall weight can be several tens of tons.

Range in patient	32 g/cm^2 maximum; 3.5 g/cm^2 minimum
Range modulation	Steps of < 0.5 g/cm^2
Range adjustment	Steps of < 0.1 g/cm^2
Average dose rate	25×25 cm^2 modulated to depth of 32 g/cm^2; dose of 2 Gy in < 1 min
Field size	Fixed > 40×40 cm^2; gantry 40×30 cm^2
Dose uniformity	2.5 %
Effective 'Source-Axis-Distance'	> 3 m
Distal dose fall-off	< 0.1 g/cm^2
Lateral penumbra	< 2 mm
Time for startup from standby	< 30 min
Time for startup from cold system	< 2 h
Time for shutdown to standby	< 10 min
Time for manual setup in one room	< 1 min
Time for automatic setup in one room	< 0.5 min
Availability	> 95%
Dosimeter reproducibility	1.5% (day); 3% (week)
Time to switch beam to rooms	< 1 min
Time to switch energy in one room	< 2 s
Radiation levels	ALARA

Table 3: Clinical specifications of the Northeast Proton Therapy Center (Flanz et al., 1995).

Treatment nozzles consist of various components for beam shaping and beam monitoring (figure 8). Beam monitoring ionization chambers detect deviations in beam position, measure the total beam current and check the beam size and uniformity. Ionization chambers may consist of parallel electrode planes divided in horizontal and vertical strips that allow the quantification of the lateral uniformity of the radiation field. These strips are integrated separately to collect the current in each strip. Such ionization chamber can be used at nozzle entrance, i.e. where the proton beam exits the beam-line, to monitors the size of the initial beam spot and the

angular distribution of the beam. Beam shaping devices in the nozzle are scatterers, absorbers, and other patient specific hardware. The nozzle also have a snout that permits mounting and positioning of the field-specific aperture and compensator along the beam axis. The snout of the nozzle is telescopic to adjust the air gap between the final collimator or compensator and the patient.

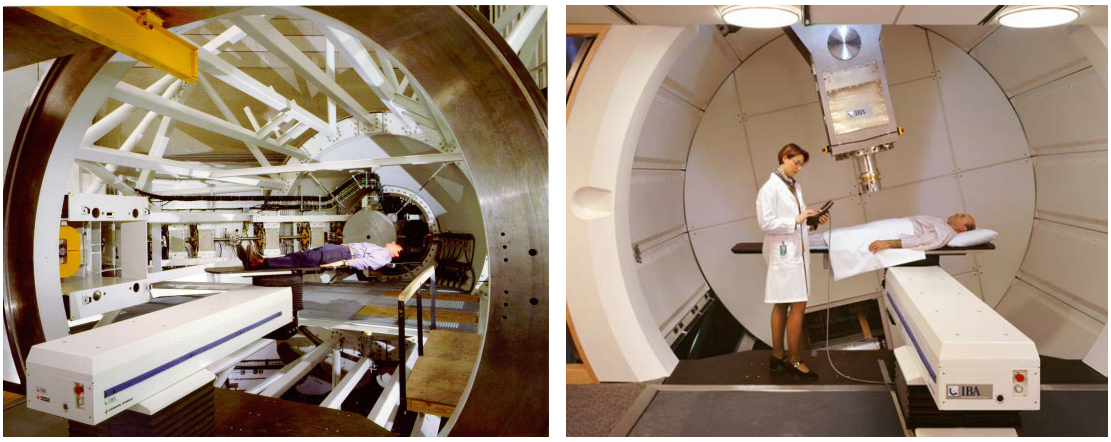

Figure 7: One of the gantries at the Northeast Proton Therapy Center. The left picture shows the gantry structure during construction with the steel assembly being visible. The right picture shows the gantry treatment room during treatment. The beam delivery nozzle is able to rotate 360 degrees around the movable patient couch. Picture provided by Ion Beam Applications, S.A.

3. Delivery Systems

a - Broad Beam (Passive Scattering)

a.1. - Scattering System

Field sizes required for tumor treatment range from as small as 1 cm up to 25 cm diameter. The field aperture has to be covered with a homogeneous particle flux. The narrow beam, with a FWHM of only about 1 cm, incident on the treatment nozzle must thus be broadened. For small fields a single scattering foil (made out of Lead) can be used to broaden the beam. For larger field sizes the reduction in proton fluence and the scattering is too big and one turns to a double-scattering system to ensure a uniform, flat lateral dose profile. The double scattering system may contain a first scatterer (set of foils), placed upstream near the nozzle entrance, and a second

gaussian-shaped scatterer placed further downstream (see figure 8). Double scattering systems have been described elsewhere (Koehler et al., 1977; Grusell et al., 1994; Paganetti et al., 2004). The second scatterer may consist of contoured bi-material scatterers. The rationale for a contoured bi-material device is that a high-Z material scatters more with little range loss whereas a low-Z material scatters less with more loss in range. In order to flatten the field the protons near the field center must be scattered more than the protons further outside the field center. This has to be achieved by maintaining the range modulation (see section 3.a.2) across the field. The contoured scatterer is approximately Gaussian shaped. The system creates a broad uniform beam at the final aperture. Key to the optimal solution for beam flattening is not only the achievable beam profile flatness but to achieve low energy loss in the absorber, thus minimizing the production of secondary radiation.

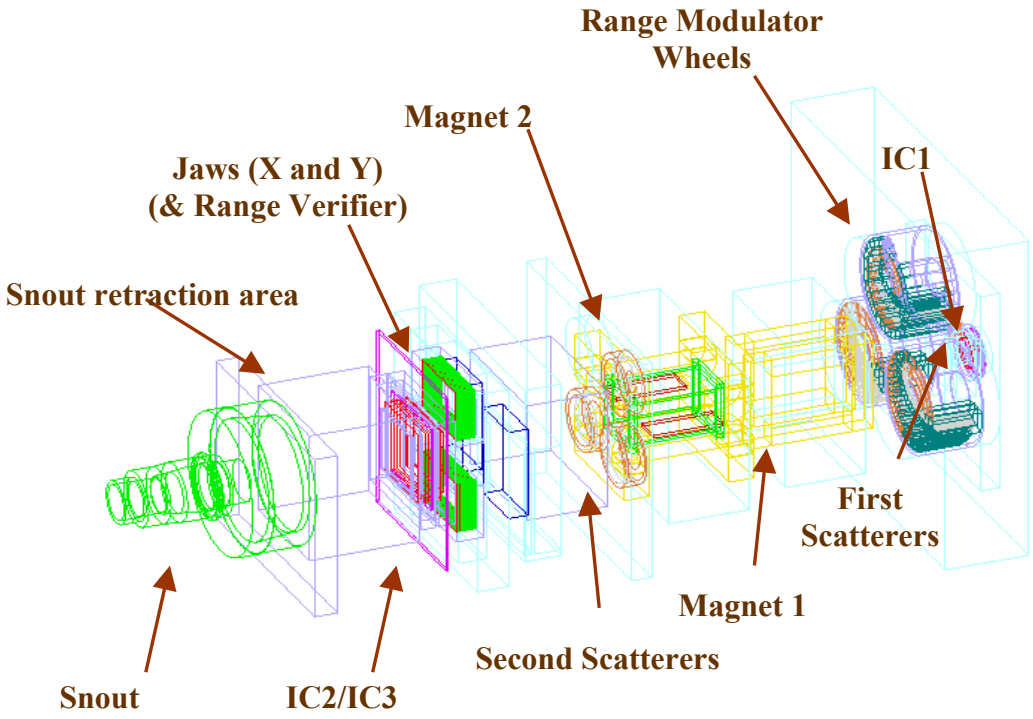

Figure 8: Schematic drawing of the nozzle at the NPTC (Paganetti et al., 2004). Beam monitoring devices are ionization chambers (IC) and a range verifier (multi-layer Faraday cup). Beam shaping devices are scattering systems, range modulators, and wobbling magnets. Variable collimators ('jaws') and the snout determine the field size.

a.2. - Range Modulator / Ridge Filter

Pristine Bragg peaks are not wide enough to cover most treatment volumes. The incident proton beam forms an SOBP by sequentially penetrating absorbers of variable thickness, e.g. via a range modulator. Each absorber contributes an individual pristine Bragg peak curve to the composite SOBP. A set of pristine peaks is delivered with decreasing depth and with reduced dose until the desired modulation is achieved. Figure 9 shows a series of weighted pristine peaks as well as the resulting SOBP when these are superimposed.

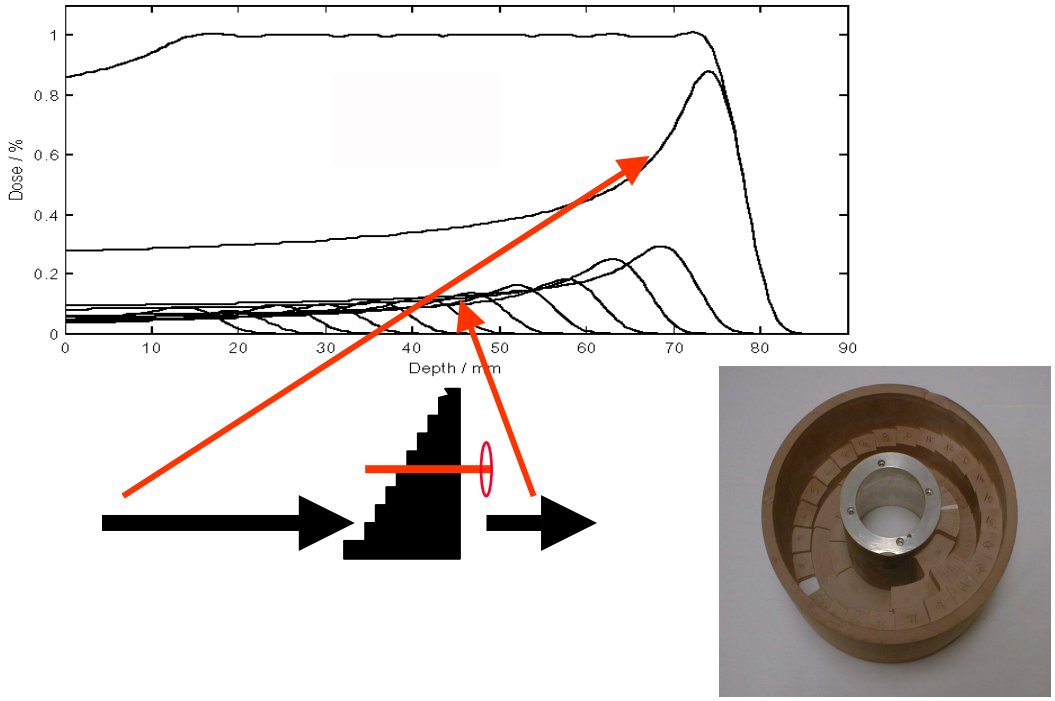

Figure 9 SOBP as composed out of a number of pristine Bragg curves modulated in depth by a set of absorbers of different thickness. The lower right picture shows a wheel with 3 different tracks used for different modulation widths.

There are different methods to modulate a field with pristine Bragg curves, e.g. modulation wheels and ridge filters (Chu et al., 1993). A modulator wheel (figure 9) combines variable thickness absorbers in circular rotating tracks that result in a temporal variation of the beam energy (Koehler et al., 1975). Such a wheel typically rotates with about 10 Hz. Modulator wheels are made of a low-Z material (Lexan or Carbon depending on the designed range interval of a wheel) and a high-Z material

(Lead). The low-Z material causes slowing down of the beam with little multiple scattering involved and high-Z material is used to adjust the amount of scattering at each depth. Each step segment of the wheel has a specific thickness and covers an angle that represents the weighting of the individual pristine Bragg curves in a SOBP. Thus, the angle covered by each step decreases with increasing absorbing power and corresponding decreased range. For small field sizes (i.e. treatment of ocular melanoma) it is sufficient to have modulator wheels made out of plastic material only.

a.3. – Aperture and Compensator

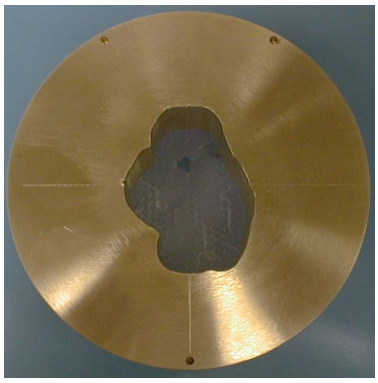

Figure 10: View of a typical brass aperture used to collimate a proton beam. (Bussiere and Adams, 2003)

Treatment fields are shaped to a desired target profile using custom milled apertures (figure 10). Apertures are often made out of Brass. It offers the best choice in terms of cost, weight and production of secondary radiation. The aperture edge, which corresponds to the 50% isodose within a port, is usually defined as the target projection to isocenter plus the 90-50% penumbra plus any set-up uncertainties.
The distal part of the dose distribution is shaped according to the desired treatment field using patient specific milled compensators (figure 11). Patient specific compensators are made out of plastic material and reduce the range of the protons. The maximum required range within a portal, usually defined as the distal 90 % of the protons, defines the thinnest point on the compensator. Each part of the compensator controls the range of the protons in its vicinity. The width of the steps can be adjusted to account for uncertainties that may affect the range at various

points along the target's cross-sectional profile. Smearing may be included to address patient setup and organ motion uncertainties.

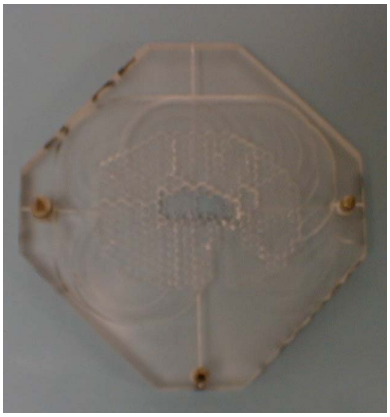

Figure 11: Top view of a range compensator made out of plastic. It is used to conform the proton dose distribution to the distal shape of a target. The various depths of the device can be seen through the transparent material.

Both aperture and compensator are mounted on a retractable snout on the treatment head. The retractable snout ensures that the air gap between the beam shaping devices and the patient can always be minimized to reduce effects of scattering in air, which causes softening of the beam penumbra (Sisterson et al., 1989).
The penumbra varies with treatment depth and beamline specific hardware settings but a typical value for 16 cm water equivalent range would be approximately 4.5 mm.

b - Scanning

Because protons can be deflected magnetically, an alternative to the use of a broad beam is to generate a narrow mono-energetic "pencil" beam and to scan it magnetically across the target volume. Typically the beam is scanned in a zigzag pattern in the x-y plane perpendicular to the beam direction. This is in close analogy to how a conventional TV set works (in which, of course, an electron beam is scanned). The depth scan (z) is done by means of energy variation. The method requires neither a collimator nor a compensator.

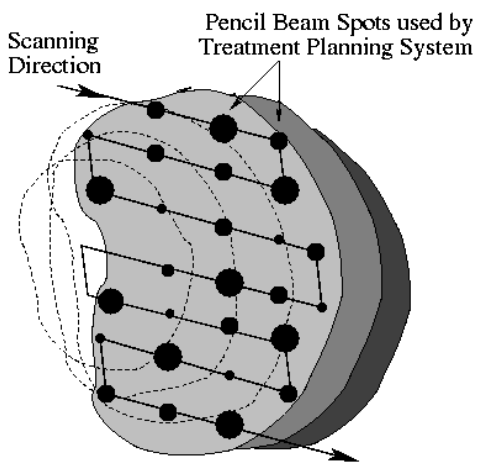

Figure 12: The principle of beam scanning: A narrow pencil beam is scanned across the target volume at various depths. The intensity can be varied from spot to spot, or continuously along the path. (Trofimov and Bortfeld, 2003)

In practice it works as follows: One starts with the deepest layer (highest energy) and does one x-y scan. The energy is then reduced, the next layer is painted, and so forth until all 20-30 layers have been delivered. Due to density variations in the patient, the Bragg peaks of one layer are not generally in a plane. Also, it is useful to keep in mind that the distal layers deliver various amounts of dose (depending on the curvature of the distal target surface) to the more proximal regions, such that each layer needs to be intensity modulated in order to generate a uniform target dose. Each layer may be delivered multiple times to reduce delivery errors and uncertainties.

Various modes of particle scanning techniques have been devised, just like different modes of photon IMRT exist:

- Discrete spot scanning: This is a step&shoot approach in which the predetermined dose is delivered to a given spot at a static position (constant magnet settings) (Kanai et al., 1980). Then the beam is switched off and the magnet settings are changed to target the next spot, dose is delivered to the next spot, and so forth (see figure 12). This approach is practically implemented at PSI in Switzerland (Pedroni et al., 1995). There the magnetic scan is performed in one direction only, and the position in the orthogonal

direction is changed through a change of the table position. Because the table motion is the slowest motion, it is the last and least often used: first the magnetic scan is performed to create one line of dose (along discrete steps), then the depth is varied by changing the energy, and another line of dose is "drawn" at a more shallow depth. This is repeated until dose is delivered at all relevant depths. Finally the table is moved to the next position, and the process is repeated.

- Raster scanning: This method, which is practically realized for heavy ions at the GSI in Darmstadt, Germany (Kraft, 2000), is very similar to discrete spot scanning, but the beam is not switched off while it moves to the next position. Practically the dose distributions are equivalent for the two methods as long as the scan time from spot to spot is small compared to the treatment time per spot. In general this is not fulfilled if the scan is done with the treatment table.
- Dynamic spot scanning: Here the beam is scanned fully continuously across the target volume. This method will be used at the NPTC. Intensity (or rather, fluence) modulation can be achieved through a modulation of the output of the source, or the speed of the scan, or both. The combination of the two reduces the required dynamic range of the source output, but puts higher demands on the control system.

One advantage of scanning is that arbitrary shapes of uniform high dose regions can be achieved with a single beam. With the broad beam technique, on the other hand, the SOBP is constant across the treatment field and typically delivers some unnecessary amount of dose proximal to the target volume. Another advantage of the scanning approach is that, due to the avoidance of first and second scatterers, the beam has less nuclear interactions outside the patient, and therefore the neutron contamination is smaller (see section 5b). The biggest advantage might be the great flexibility, which can be fully utilized in intensity-modulated proton therapy (IMPT), as we will explain below. However, a disadvantage is the technical difficulty to generate very narrow pencil beams that result in an optimal lateral dose fall-off. The scanning approach can also be more sensitive to organ motion than passive scattering (Phillips et al., 1992; Bortfeld et al., 2002).

Another variant of scanning is called "wobbling". Here a relatively broad beam (diameter in the order 5 cm) is magnetically scanned across the target volume. Because this would result in a broad penumbra, collimators are still required. The main advantage is that larger field sizes than with passive scattering are easily achievable.

4. Proton-Specific Treatment Planning

a - Broad Beam

a.1. - Standard Techniques

There are different vendors that offer treatment planning systems for proton beam therapy. The software packages are either designed for proton therapy planning only or are able to generate plans for conventional photon therapy as well as proton therapy. Different algorithms can be used to calculate dose in the patient. In a broad beam ray-tracing model the SOBP portion of a depth dose is set to 100% and generic functions are used to describe the proximal build-up as well as the distal fall-off. Lateral penumbra functions are used to form the lateral profiles of beams. With the advent of faster computers more complex and much more accurate pencil beam models have become the norm replacing the broad beam model. Pencil beam algorithms rely on pencil kernels, derived from physical treatment machine data, to model proton range mixing from scatter in the range compensator and patient (Goitein and Miller, 1983). The calculated proximal build-up, distal fall-off and lateral penumbra are usually in good agreement with measurements (Hong et al., 1996). In addition to ray-tracing or pencil-beam algorithms there are Monte Carlo dose calculation procedures used mainly in research. They are believed to be more accurate (Pawlicki and Ma, 2001) but usually take too much computing time to be used in routine treatment planning. Monte Carlo dose calculation for proton therapy treatment planning is currently under development (Jiang and Paganetti, 2004; Paganetti et al., 2004).

As with photons and electrons proton treatments use multiple portals to reduce the overall skin dose to patients. Because proton beams have a sharp distal fall-off it is possible to aim beams towards critical structures in treatment planning. Thus,

treatment strategies and treatment options can be different from conventional therapy. The sharp distal dose fall-off of protons (distance from the 90% to the 10% dose level is only a few mm) makes it more critical than with photons to understand and limit the uncertainties used in determining the penetration depth required to cover a target. The uncertainties must be incorporated in the treatment planning margins around the target volume. The accuracy of proton beam delivery may in general allow tighter margins than used conventionally. However, one has to keep in mind that higher accuracy also means that dose delivery is more affected by uncertainties caused by beam delivery, patient setup and immobilization, tissue heterogeneities, and organ motion.

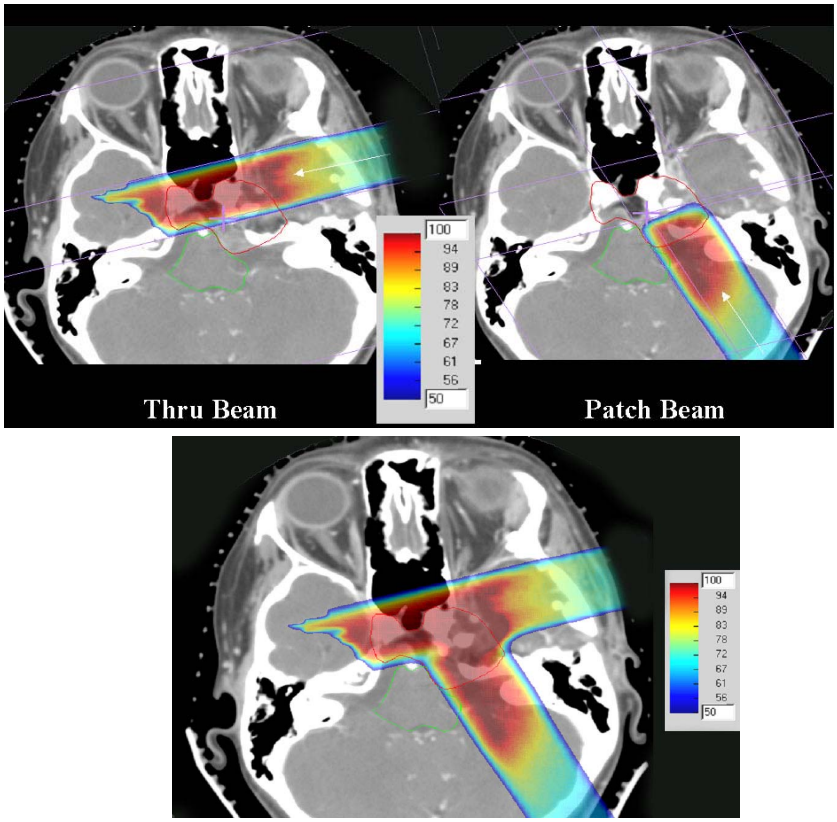

Figure 13: Axial CT image with color-wash dose display resulting from thru-field which irradiates the anterior portion of the target while avoiding the brainstem and patch-field which treats the remaining portion of the target while avoiding the brainstem. The lower figure shows the combined thru/patch field combination. All doses are given in percent. (Bussiere and Adams, 2003)

Imaging studies prior to treatment-planning and the process of delineating target volumes and structures of interest are identical in proton therapy and in conventional therapy. However, planning and delivery strategies may be different. Typical head and neck cases include four to six non-coplanar fields. During a treatment session between one and three fields are treated. The fields are alternated for subsequent treatment sessions to distribute the daily non-target dose (Bussiere and Adams, 2003).

A dose delivery strategy unique to particle therapy is called "patching". Two fields are combined such that the first field treats a segment of the target avoiding a nearby critical organ with the lateral penumbra. The second field treats the remaining segment, also avoiding the critical organ with the lateral penumbra and matching it's distal fall-off 50% dose with the other field's lateral penumbra's 50% dose value. Because of tissue heterogeneity it can be difficult to obtain a uniform dose along the patch junction. Therefore, patch junctions are always selected to be within the target volume. One allows overshoot of the patch field to minimize the low dose region. Using a combination of patch fields with different junctions ensures that the magnitude of the low and high dose regions is acceptable. Figure 13 shows a typical patch field combination for a skull base tumor (Bussiere and Adams, 2003).

b - Scanning and IMPT

The recent advances in IMRT have challenged proton therapy. Treatment planning comparison studies have shown that IMRT can produce dose distributions that are comparable with proton distributions in terms of target conformality and dose gradients in the high-dose region (Lomax et al., 1999). In some cases, IMRT produces even more target-conformal dose distributions in the high-dose region than protons. In the low to medium dose region and in terms of integral dose, protons are, however, always better. Nevertheless, it is somewhat questionable if the higher cost of proton therapy is justifiable if integral dose was the only advantage of protons.

The study mentioned above compares IMRT photon therapy with conventional passive scattering proton techniques. The dose conforming potential of the latter is limited and this has mainly technical reasons; it has nothing to do with the physical dose conformation potential of protons. To fully exploit the physical potential of

proton therapy and to permit a fair comparison with IMRT, intensity modulation techniques have to be introduced into proton therapy as well. This is then called IMPT, intensity modulated proton therapy. The name is somewhat misleading because intensity modulation is always required in proton therapy, even for the generation of an SOBP. What we mean by IMPT is a treatment technique that, in analogy with IMRT, delivers intentionally non-uniform dose distributions from each treatment field at a given direction. The desired (generally uniform) dose in the target volume is obtained after superimposing the dose contributions from all fields. The additional degrees of freedom (by not having to produce uniform dose from each direction) can be used to optimize dose distributions in several ways, which we will now describe.

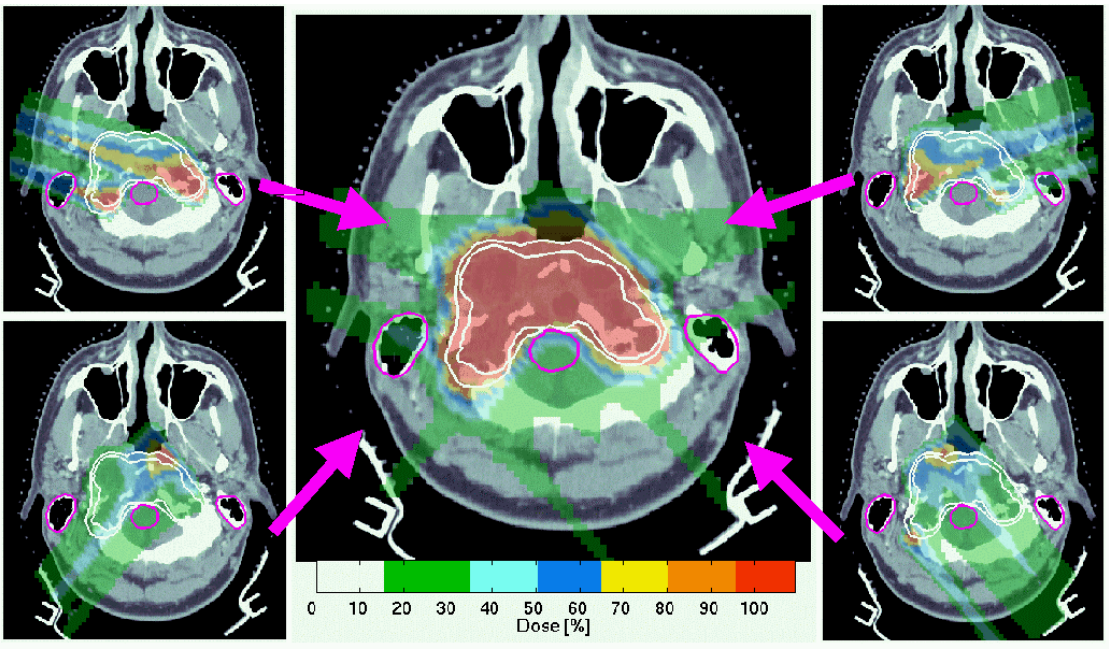

Figure 14: The principle of intensity modulated proton therapy (IMPT). Non-uniform dose distributions from a number of fields (4 in this case) yield the desired (uniform) target dose. Figure provided by Alex Trofimov (Massachusetts General Hospital).

IMPT treatment plans are optimized using an "inverse" treatment planning system, which is similar to inverse planning for photon IMRT (Oelfke and Bortfeld, 2001). The main difference is that in IMPT the energy of each pencil beam can be varied in addition to its intensity. This increases the number of degrees of freedom drastically,

which increases its dose shaping potential but also increases the computational and delivery complexity. The calculation can be simplified and the solution be steered in the desired direction if certain IMPT techniques are pre-selected. Lomax has summarized various IMPT techniques whose complexities are between the conventional passive scattering technique and the most general ("3D") technique. One of the simpler techniques is the 2.5D technique, which is actually quite similar to IMRT. It uses poly-energetic SOBP pencil beams, which are individually adapted to the proximal and distal edge of the target volume (figure 14), such that the dose is constant along the depth of the target volume. The weights (i.e., intensities) of the SOBP pencil beams are modulated across the target volume (symbolized by different colors in figure 15).

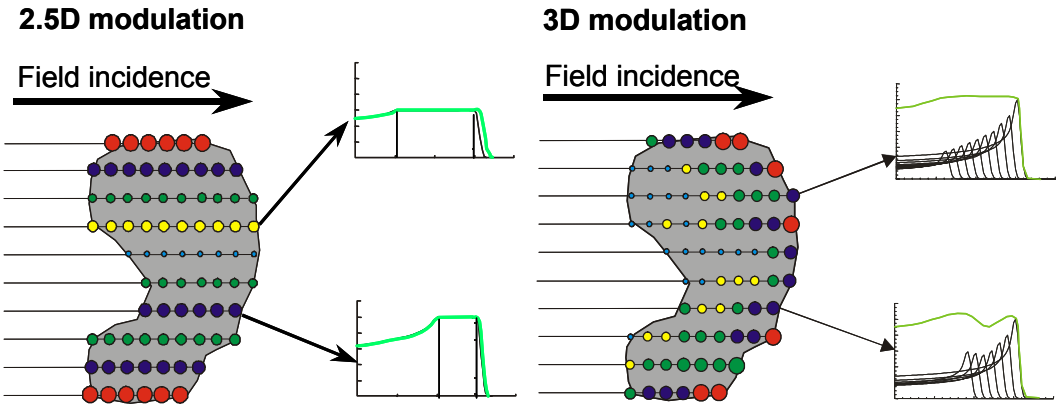

Figure 15: Comparison of the 2.5D IMPT modulation technique with the most general 3D approach. Different weights are symbolized by different colors. (Lomax, 1999)

Another technique was devised by Deasy et al. (Deasy et al., 1997) and is called distal edge tracking (DET). As indicated by its name, it puts Bragg peaks on the distal edge of the target volume only and thereby creates a highly non-uniform dose per treatment field. The desired uniform dose is obtained by superimposing multiple fields from different directions, in combinations with optimized intensity modulation. The DET technique produces the smallest possible integral dose because every constituent pencil beam delivers the best possible ratio between target dose and dose to the proximal normal structures. Moreover, the DET technique yields very sharp dose gradients because it shapes the dose distribution mainly with the

distal edge of the Bragg peak, which is sharper than the lateral fall-off (as long as the energy spectrum is not too wide). However, for obvious reasons DET has greater difficulties in generating a high uniformity of the target dose. Also, it is more sensitive to range uncertainties than, for example, the 2.5D technique (figure 15). Furthermore, shaping dose distributions with the distal edge of the Bragg peak with its high LET and RBE may raise some biological flags (Wilkens and Oelfke, 2004) (see section on RBE).

In summary, IMPT treatments can be tailored to yield one of the following advantages:

- improved dose conformality and steeper dose gradients,
- further reduction of integral dose,
- less sensitivity to range uncertainties and other sources of uncertainty (Lomax et al., 2001),

or a combination thereof. However, not all of them may be achievable at the same time to the full extent.

5. Biological effectiveness

a - RBE

Protons are slightly more biologically effective than photons. In other words, lower dose is required to cause the same biological effect. The relative biological effectiveness (RBE) of protons is defined as the dose of a reference radiation divided by the proton dose to achieve the same biological effect. The fundamental reason for applying a RBE value is to ensure that radiation oncologists can benefit from the large pool of clinical results obtained with photon beams. The RBE adjusted dose is defined as the product of the physical dose and the respective RBE describing the radiosensitivity of the tissue after ion irradiation compared to photon irradiation at a given level of effect. Proton therapy is based on the use of a single RBE value (equals 1.1 at almost all institutions), which is applied to all proton beam treatments independent of dose/fraction, position in the SOBP, initial beam energy or the particular tissue. A generic RBE is only a rough approximation considering experimentally determined RBE's for both in vitro and in vivo systems (Paganetti et

al., 2002; Paganetti, 2003). Dependencies of the RBE on various physical and biological properties are disregarded. The RBE of principal concern is that of the critical normal tissue/organ(s) immediately adjacent to or within the treatment volume, i.e. the determinant(s) of NTCP.

Although the fact that a generic RBE cannot be the true RBE for each tissue, dose/fraction etc. has long been recognized, it was concluded that the magnitude of RBE variation with treatment parameters is small relative to our abilities to determine RBE values (Paganetti and Goitein, 2001; Paganetti, 2003). The variability of RBE in clinical situations is believed to be within 10-20%. The values for cell survival in vitro indicate a substantial spread between the diverse cell lines. The average value at mid SOBP over all dose levels was shown to be ≈1.2 in vitro and ≈1.1 in vivo (Paganetti et al., 2002). Both in vitro and in vivo data indicated a small but statistically significant increase in RBE for lower doses per fraction, which is much smaller for in vivo systems. Evaluation of the statistically significant difference in RBE between in vitro and in vivo systems should deal explicitly with the fact that the former uses as the end-point the killing of single cells of one cell population (colony formation). The in vivo response reflects the more complex expression of the integrated radiation damage to several tissue systems (cell populations). In addition, the in vivo data refer to various different biological processes (e.g., mutation). The dependency on dose, i.e. increasing RBE with decreasing dose, appears to be far less in vivo compared to the in vitro data. Unfortunately, RBE values from in vivo systems at doses of < 4Gy are quite limited.

The effect of radiation on cells and tissues is a complex and not entirely understood function of the properties of the cell or tissue and the microdosimetric properties of the radiation field. The dependencies of RBE on biological endpoint and dose are difficult to explain microscopically. However, the LET dependency can be explained based on the concept that ionization density within the sensitive cellular structure (e.g. DNA) increases with LET and that production of non-reparable lesions increases with ionization density. For constant conditions at irradiation a change in response of a cell population to a defined physical dose by different radiation beams is generally accepted as due to differences in LET. Mean LET is only one parameter, which characterizes that microdosimetric structure, and it is only one of several

determinants of radiation response. In general as LET increases, the RBE increases, eventually reaching a maximum and then decreasing (Goodhead, 1990). Based on these considerations a small increase in the proton RBE across the SOBP and the extension of the penetration of the beam by a few mm is expected because of an increasing LET (Paganetti et al., 1997; Paganetti, 1998; Paganetti and Goitein, 2000; Wilkens and Oelfke, 2004). Calculations show that LET increases slightly throughout the SOBP and significantly at the terminal end of a SOBP. This measurable increase in RBE over the terminal few mm of the SOBP results in an extension of the bio-effective range of the beam of a few mm (Robertson et al., 1975; Wouters et al., 1996; Paganetti and Goitein, 2000). This needs to be considered in treatment planning, particularly for single field plans or for an end of range in or close to a critical structure. Clinicians and treatment planners are often reluctant to having the SOBP abutting a critical structure thus not utilizing one advantage of protons, namely the sharp distal fall-off.

b - Secondary Radiation

Protons slowing down in matter loose energy not only by coulomb interactions but also by nuclear interactions (Laitano et al., 1996; Medin and Andreo, 1997; Paganetti, 2002). Nuclear interactions cause secondary radiation. Protons and neutrons are the most important secondary particles from nuclear interactions because they can carry away energy far from the interaction point. Shielding against neutron radiation is therefore important for any proton therapy installation. For example, different combinations of apertures may be used in the treatment head. However, neutron production can not be avoided. Shielding may reduce the effect of neutrons generated in the scattering system, the aperture and the compensator but neutrons are also generated in the patient itself. Nothing can be done to avoid the latter. Since the total amount of neutrons produced depends on the amount of material the protons have to penetrate, neutron production can be reduced by extracting to the nozzle the minimum energy needed.

6. Patient Positioning & Immobilization Issues, Motion

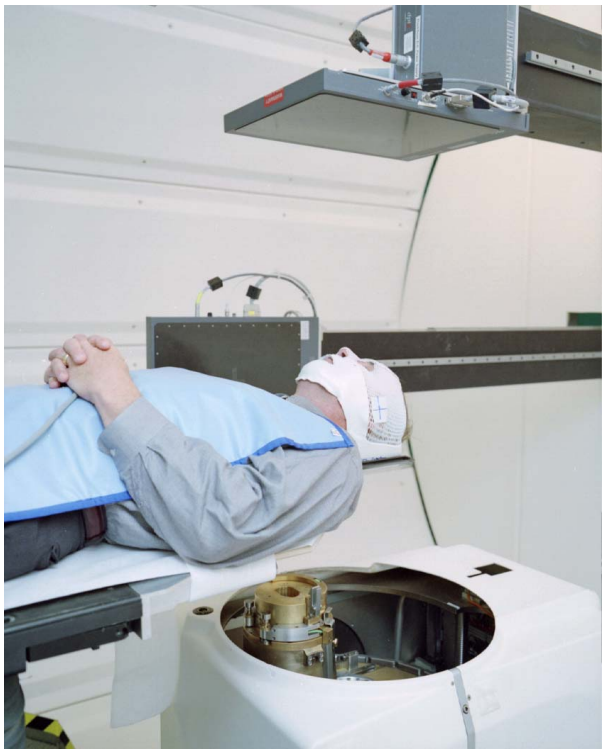

Figure 16: Proton therapy requires, like all highly conformal treatment modalities, a significant effort in patient setup and immobilization. This figure shows the setup at NPTC using orthogonal x-rays (one x-ray source is integrated into the nozzle) and flat panel detectors. Picture provided by Skip Rosenthal (Massachusetts General Hospital)

Proton therapy is, like all highly target-conformal treatment modalities, susceptible to geographical misses. Considerable effort is therefore necessary to position and immobilize the patient. For example, at the NPTC orthogonal X-ray projections are used to detect both translational and rotational positioning errors and correct those errors using a 6 axes table within 1 mm or 0.5 degrees (figure 16). For the most part, positioning and immobilization issues are identical for proton therapy and, for example, IMRT. However, there are a few issues that are specific to protons and other charged particles. They have to do with the simple fact that the range is affected by structures moving in and out of the beam. For example, in prostate treatments the position of the Bragg peak may be significantly altered if parts of the pelvic bone move into the beam, which can happen if on one treatment day the pelvis is rotated compared to the planned position (Phillips et al., 2002). Similar problems can affect treatments in the skull (figure 16). Therefore, in particle therapy it is not

only important to ensure that the target volume is always at the same position, but the surrounding structures and especially bony structures should also be at their planned position. The detrimental effect of misalignments can be mitigated to some degree in treatment planning. A common approach in passive scattering proton therapy is to "smear" (thin) the range compensator such that target coverage is ensured even if the position is slightly off. However, this will push the dose into the normal tissues distal to the target volume and the smearing radius is therefore limited to about 3 mm. Bigger errors cannot be compensated with this method.

Besides alignment errors, proton (and charged particle) therapy is also uniquely affected by internal organ motion, especially in the case of lung tumors. The dose distribution is deformed by the motion of the tumor in the low density lung tissue . Unless methods such as gating (Minohara et al., 2000) are used to "freeze" the motion, this effect must be carefully considered at treatment planning stage. This is doable (Moyers et al., 2001) but it is fair to say the proton treatments of lung tumors have not fully come of age yet.

7. References

Archambeau JO, Slater JD, Slater JM, Tangeman R. 1992. Role for proton beam irradiation in treatment of pediatric CNS malignancies. International Journal of Radiation Oncology, Biology, Physics 22:287-294.

Benk V, Liebsch NJ, Munzenrider JE, Efird J, McManus P, Suit H. 1995. Base of skull and cervical spine chordomas in children treated by high-dose irradiation. 31.

Blosser H, Bailey J, Burleigh R, Johnson D, Kashy E, Kuo T, Marti F, Vincent J, Zeller A, Blosser E, Blosser G, Maughan R, Power W, Wagner J. 1989. Superconducting Cyclotron for Medical Applications. IEEE Transactions on Magnetics 25:1746-1754.

Bortfeld T, Jokivarsi K, Goitein M, Kung J, Jiang SB. 2002. Effects of intra-fraction motion on IMRT dose delivery: Statistical analysis and simulation. Physics in Medicine and Biology 47:2303-2320.

Bussiere MR, Adams JA. 2003. Treatment planning for conformal proton radiation therapy. Technology in Cancer Research & Treatment 2:389-399.

Chu WT, Ludewigt BA, Renner TR. 1993. Instrumentation for treatment of cancer using proton and light-ion beams. Review of Scientific Instruments 64:2055-2122.

Coutrakon G, Slater JM, Ghebremedhin A. 1999. Design considerations for medical proton accelerators. Proceedings of the 1999 Particle Accelerator Conference, New York:11-15.

Cozzi L, Fogliata A, Lomax A, Bolsi A. 2001. A treatment planning comparison of 3D conformal therapy, intensity modulated photon therapy and proton therapy fot treatment of advanced head and neck tumours. Radiotherapy and Oncology 61:287-297.

Deasy JO, Shepard DM, Mackie TR. 1997. Distal edge tracking: A pro-posed delivery method for conformal proton therapy using intensity modula-tion. D.D. Leavitt and G. Starkschall, editors, XIIth International Confer-ence on the Use of Computers in Radiation Therapy, Madison, 1997. Medical Physics Publishing:406-409.

Delaney TF, Smith AR, Lomax A, Adams J, Loeffler JS. 2003. Proton Beam Radiation Therapy. Cancer Principles & Practice of Oncology 17:1-10.

Flanz J, Durlacher S, Goitein M, Levine A, Reardon P, Smith A. 1995. Overview of the MGH-Northeast Proton Therapy Center plans and progress. Nuclear Instruments and Methods in Physics Research B 99:830-834.

Fuss M, Hug EB, Schaefer RA, Nevinny-Stickel M, Miller DW, Slater JM, Slater JD. 1999. Proton radiation therapy (PRT) for pediatric optic pathway gliomas: Comparison with 3D planned conventional photons and a standard photon technique. International Journal of Radiation Oncology, Biology, Physics 45:1117-1126.

Fuss M, Poljanc K, Miller DW, Archambeau JO, Slater JM, Slater JD, Hug EB. 2000. Normal tissue complication probability (NTCP) calculations as a means to compare proton and photon plans and evaluation of clinical appropriateness of calculated values. International Journal of Cancer (Radiat. Oncol. Invest) 90:351-358.

Goitein M, Jermann M. 2003. The relative costs of proton and X-ray radiation therapy. Clinical Oncology 15:S37-50.

Goitein M, Miller T. 1983. Planning proton therapy of the eye. Medical Physics 10:275-283.

Goodhead DT. 1990. Radiation effects in living cells. Canadian Journal of Physics 68:872-886.

Grusell E, Montelius A, Brahme A, Rikner G, Russell K. 1994. A general solution to charged particle beam flattening using an optimized dual-scattering-foil technique, with application to proton therapy beams. Physics in Medicine and Biology 39:2201-2216.

Hara I, Murakami M, Kagawa K, Sugimura K, Kamidono S, Hishikawa Y, Abe M. 2004. Experience with conformal proton therapy for early prostate cancer. American Journal of Clinical Oncology 27:323-327.

Harsh G, Loeffler JS, Thornton A, Smith A, Bussiere M, Chapman PH. 1999. Stereotactic proton radiosurgery. Neurosurgery Clinics of North America 10:243-256.

Hong L, Goitein M, Bucciolini M, Comiskey R, Gottschalk B, Rosenthal S, Serago C, Urie M. 1996. A pencil beam algorithm for proton dose calculations. Physics in Medicine and Biology 41:1305-1330.

Hug EB, Devries A, Thornton AF, Munzenrider JE, Pardo FS, Hedley-Whyte ET, Bussiere MR, Ojemann R. 2000. Management of atypical and malignant meningiomas: role of high-dose, 3D-conformal radiation therapy. Journal of Neuro-Oncology 48:151-160.

Hug EB, Fitzek MM, Liebsch NJ, Munzenrider JE. 1995. Locally challenging osteo- and chondrogenic tumors of the axial skeleton: Results of combined proton and photon radiation therapy using three-dimensional treatment planning. International Journal of Radiation Oncology, Biology, Physics 31:467-476.

Hug EB, Slater JD. 1999. Proton radiation therapy for pediatric malignancies: status report. Strahlentherapie und Onkologie 175; Supplement 2:89-91.

Isacsson U, Hagberg H, Johansson K-A, Montelius A, Jung B, Glimelius B. 1997. Potential advantages of protons over conventional radiation beams for paraspinal tumours. Radiotherapy and Oncology 45:63-70.

Isacsson U, Lennernäs B, Grusell E, Jung B, Montelius A, Glimelius B. 1998. Comparative treatment planning between proton and X-ray therapy in esophageal cancer. International Journal of Radiation Oncology, Biology, Physics 41:441-450.

Isacsson U, Montelius A, Jung B, Glimelius B. 1996. Comparative treatment planning between proton and X-ray therapy in locally advanced rectal cancer. Radiotherapy and Oncology 41:263-272.

Jiang H, Paganetti H. 2004. Adaptation of GEANT4 to Monte Carlo dose calculations based on CT data. Medical Physics in press.

Kanai T, Kawachi K, Kumamoto Y, Ogawa H, Yamada T, Matsuzawa H, Inada T. 1980. Spot scanning system for proton radiotherapy. Medical Physics 7:365-369.

Koehler AM, Schneider RJ, Sisterson JM. 1975. Range Modulators for Protons and Heavy Ions. Nuclear Instruments and Methods 131:437-440.

Koehler AM, Schneider RJ, Sisterson JM. 1977. Flattening of proton dose distributions for large-field radiotherapy. Medical Physics 4:297-301.

Kraft G. 2000. Tumortherapy with ion beams. Nuclear Instruments and Methods in Physics Research A 454:1-10.

Laitano RF, Rosetti M, Frisoni M. 1996. Effects of nuclear interactions on energy and stopping power in proton beam dosimetry. Nuclear Instruments and Methods A 376:466-476.

Lee M, Wynne C, Webb S, Nahum AE, Dearnaley D. 1994. A comparison of proton and megavoltage X-ray treatment planning for prostate cancer. Radiotherapy and Oncology 33:239-253.

Levin CV. 1992. Potential for gain in the use of proton beam boost to the para-aortic lymph nodes in carcinoma of the cervix. International Journal of Radiation Oncology, Biology, Physics 22:355-359.

Lin R, Hug EB, Schaefer RA, Miller DW, Slater JM, Slater JD. 2000. Conformal Proton radiation Therapy of the Posterior Fossa: A Study Comparing Protons with Three-Dimensional Planned Photons in Limiting Dose to Auditory Structures. International Journal of Radiation Oncology, Biology, Physics 48:1219-1226.

Lomax A. 1999. Intensity modulation methods for proton radiotherapy. Physics in Medicine and Biology 44:185-205.

Lomax AJ, Boehringer T, Coray A, Egger E, Goitein G, Grossmann M, Juelke P, Lin S, Pedroni E, Rohrer B, Roser W, Rossi B, Siegenthaler B, Stadelmann O, Stauble H, Vetter C, Wisser L. 2001. Intensity modulated proton therapy: A clinical example. Medical Physics 28:317-324.

Lomax AJ, Bortfeld T, Goitein G, Debus J, Dykstra C, Tercier P-A, Coucke PA, Mirimanoff RO. 1999. A treatment planning inter-comparison of proton and intensity modulated photon radiotherapy. Radiotherapy and Oncology 51:257-271.

Lomax AJ, Cella L, Weber D, Kurtz JM, Miralbell R. 2003. Potential role of intensity-modulated photons and protons in the treatment of the breast and regional nodes. International Journal of Radiation Oncology, Biology, Physics 55:785-792.

Lomax AJ, Goitein M, Adams J. 2003. Intensity modulation in radiotherapy: photons versus protons in the paranasal sinus. Radiotherapy and Oncology 66:11-18.

McAllister B, Archambeau JO, Nguyen MC, Slater JD, Loredo L, Schulte R, Alvarez O, Bedros AA, Kaleita T, Moyers M, Miller D, Slater JM. 1997. Proton therapy for pediatric cranial tumors: preliminary report on treatment and disease-related morbidities. International Journal of Radiation Oncology, Biology, Physics 39:455-460.

Medin J, Andreo P. 1997. Monte Carlo calculated stopping-power ratios, water/air, for clinical proton dosimetry (50-250 MeV). Physics in Medicine and Biology 42:89-105.

Minohara S, Kanai T, Endo M, Noda K, Kanazawa M. 2000. Respiratory gated irradiation system for heavy-ion radiotherapy. International Journal of Radiation Oncology, Biology, Physics 47:1097-1103.

Miralbell R, Crowell C, Suit HD. 1992. Potential improvement of three dimension treatment planning and proton therapy in the outcome of maxillary sinus cancer. International Journal of Radiation Oncology, Biology, Physics 22:305-310.

Miralbell R, Lomax A, Russo M. 1997. Potential role of proton therapy in the treatment of pediatric medulloblastoma/primitive neuro-ectodermal tumors: Spinal theca irradiation. International Journal of Radiation Oncology, Biology, Physics 38:805-811.

Moyers MF, Miller DW, Bush DA, Slater JD. 2001. Methodologies and tools for proton beam design for lung tumors. International Journal of Radiation Oncology, Biology, Physics 49:1429-1438.

Niemierko A, Urie M, Goitein M. 1992. Optimization of 3D Radiation Therapy with both Physical and Biological End Points and Constraints. International Journal of Radiation Oncology, Biology, Physics 23:99-108.

Nowakowski VA, Castro JR, Petti PL, Collier JM, Daftari I, Ahn D, Gauger G, Gutin P, Linstadt DE, Phillips TL. 1992. Charged particle radiotherapy of paraspinal tumors. International Journal of Radiation Oncology, Biology, Physics 22:295-303.

Oelfke U, Bortfeld T. 2001. Inverse Planning for Photon and Proton Beams. Medical Dosimetry 26:113-124.

Paganetti H. 1998. Calculation of the spatial variation of relative biological effectiveness in a therapeutic proton field for eye treatment. Physics in Medicine and Biology 43:2147-2157.

Paganetti H. 2002. Nuclear Interactions in Proton Therapy: Dose and Relative Biological Effect Distributions Originating From Primary and Secondary Particles. Physics in Medicine and Biology 47:747-764.

Paganetti H. 2003. Significance and implementation of RBE variations in proton beam therapy. Technology in Cancer Research & Treatment 2:413-426.

Paganetti H, Goitein M. 2000. Radiobiological significance of beam line dependent proton energy distributions in a spread-out Bragg peak. Medical Physics 27:1119-1126.

Paganetti H, Goitein M. 2001. Biophysical Modeling of Proton Radiation Effects Based on Amorphous Track Models. International Journal of Radiation Biology 77:911-928.

Paganetti H, Jiang H, Adams JA, Chen GT, Rietzel E. 2004. Monte Carlo simulations with time-dependent geometries to investigate organ motion with high temporal resolution. International Journal of Radiation Oncology, Biology, Physics in press.

Paganetti H, Jiang H, Lee S-Y, Kooy H. 2004. Accurate Monte Carlo for nozzle design, commissioning, and quality assurance in proton therapy. Medical Physics 31:2107-2118.

Paganetti H, Niemierko A, Ancukiewicz M, Gerweck LE, Loeffler JS, Goitein M, Suit HD. 2002. Relative biological effectiveness (RBE) values for proton beam therapy. International Journal of Radiation Oncology, Biology, Physics 53:407-421.

Paganetti H, Olko P, Kobus H, Becker R, Schmitz T, Waligorski MPR, Filges D, Mueller-Gaertner HW. 1997. Calculation of RBE for Proton beams Using Biological Weighting Functions. International Journal of Radiation Oncology, Biology, Physics 37:719-729.

Pawlicki T, Ma C-MC. 2001. Monte Carlo simulation for MLC-based intensity-modulated radiotherapy. Medical Dosimetry 26:157-168.

Pedroni E, Bacher R, Blattmann H, Boehringer T, Coray A, Lomax A, Lin S, Munkel G, Scheib S, Schneider U, Tourovsky A. 1995. The 200-MeV proton therapy project at the Paul Scherrer Institute: Conceptual design and practical realization. Medical Physics 22:37-53.

Phillips BL, Jiroutek MR, Tracton G, Elfervig M, Muller KE, Chaney EL. 2002. Thresholds for human detection of patient setup errors in digitally reconstructed portal images of prostate fields. International Journal of Radiation Oncology, Biology, Physics 54:270-277.

Phillips MH, Pedroni E, Blattmann H, Boehringer T, Coray A, Scheib S. 1992. Effects of respiratory motion on dose uniformity with a charged particle scanning method. Physics in Medicine and Biology 37:223-234.

Robertson JB, Williams JR, Schmidt RA, Little JB, Flynn DF, Suit HD. 1975. Radiobiological Studies of a High-Energy Modulated Proton Beam Utilizing Cultured Mammalian Cells. Cancer 35:1664-1677.

Rosenberg AE, Nielsen GP, Keel SB, Renard LG, Fitzek MM, Munzenrider JE, Liebsch NJ. 1999. Chondrosarcoma of the base of the skull: a clinicopathologic study of 200 cases with emphasis on its distinction from chordoma. American Journal of Surgical Pathology 23:1370-1378.

Shioyama Y, Tokuuye K, Okumura T, Kagei K, Sugahara S, Ohara K, Akine Y, Ishikawa S, Satoh H, Sekizawa K. 2003. Clinical evaluation of proton radiotherapy for non-small-cell lung cancer. International Journal of Radiation Oncology, Biology, Physics 56:7-13.

Sisterson JM. 2004. Particles Newsletter. http://ptcog.mgh.harvard.edu/.

Sisterson JM, Urie MM, Koehler AM, Goitein M. 1989. Distal penetration of proton beams: the effects of air gaps between compensating bolus and patient. Physics in Medicine and Biology 34:1309-1315.

Slater JD, Rossi CJJ, Yonemoto LT, Bush DA, Jabola BR, Levy RP, Grove RI, Preston W, Slater JM. 2004. Proton therapy for prostate cancer: the initial Loma Linda University experience. International Journal of Radiation Oncology, Biology, Physics 59:348-352.

Slater JD, Slater JM, Wahlen S. 1992. The potential for proton beam therapy in locally advanced carcinoma of the cervix. International Journal of Radiation Oncology, Biology, Physics 22:343-347.

Slater JM, Slater JD, Archambeau JO. 1992. Carcinoma of the tonsillar region: potential for use of proton beam therapy. International Journal of Radiation Oncology, Biology, Physics 22:311-319.

Smit BM. 1992. Prospects for proton therapy in carcinoma of the cervix. International Journal of Radiation Oncology, Biology, Physics 22:349-353.

Tatsuzaki H, Urie MM, Linggood R. 1992. Comparative treatment planning: proton vs. X-ray beams against glioblastoma multiforme. International Journal of Radiation Oncology, Biology, Physics 22:265-273.

Tatsuzaki H, Urie MM, Willett CG. 1992. 3-D comparative study of proton vs. X-ray radiation therapy for rectal cancer. International Journal of Radiation Oncology, Biology, Physics 22:369-374.

Terahara A, Niemierko A, Goitein M, Finkelstein D, Hug E, Liebsch N, O'Farrell D, Lyons S, Munzenrider J. 1999. Analysis of the relationship between tumor dose inhomogeneity and local control in patients with skull base chordoma. International Journal of Radiation Oncology, Biology, Physics 45:351-358.

Thornton A, Fitzek M, Varvares M, Adams J, Rosenthal S, Pollock S, Jackson M, Pilch B, Joseph M. 1998. Accelerated Hyperfractionated Proton/Photon Irradiation for Advanced Paranasal Sinus Cancer, Results of a Perspective Phase I-II Study. International Journal of Radiation Oncology, Biology, Physics 42 Supplement:222.

Tobias CA, Lawrence JH, Born JL, McCombs R, Roberts JE, Anger HO, Low-Beer BVA, Huggins C. 1958. Pituitary Irradiation with High Energy Proton Beams: a Preliminary Report. Cancer Research 18:121-134.

Trofimov A, Bortfeld T. 2003. Optimization of Beam Parameters and Treatment Planning for Intensity Modulated Proton Therapy. Technology in Cancer Research & Treatment 2:437-444.

Wambersie A, Gregoire V, Brucher J-M. 1992. Potential clinical gain of proton (and heavy ion) beams for brain tumors in children. International Journal of Radiation Oncology, Biology, Physics 22:275-286.

Weber DC, Trofimov AV, Delaney TF, Bortfeld T. 2004. A treatment plan comparison of intensity modulated photon and proton therapy for paraspinal sarcomas. International Journal of Radiation Oncology, Biology, Physics 58:1596-1606.

Wenkel E, Thornton AF, Finkelstein D, Adams J, Lyons S, De La Monte S, Ojeman RG, Munzenrider JE. 2000. Benign meningioma: Partially resected, biopsied, and recurrent intracranial tumors treated with combined proton and photon radiotherapy. International Journal of Radiation Oncology, Biology, Physics 48:1363-1370.

Wilkens JJ, Oelfke U. 2004. A phenomenological model for the relative biological effectiveness in therapeutic proton beams. Physics in Medicine and Biology 49:2811-2825.

Wilson RR. 1946. Radiological Use of Fast Protons. Radiology 47:487-491.

Wouters BG, Lam GKY, Oelfke U, Gardey K, Durand RE, Skarsgard LD. 1996. RBE Measurement on the 70 MeV Proton Beam at TRIUMF using V79 cells and the High Precision Cell Sorter Assay. Radiation Research 146:159-170.

Yeboah C, Sandison GA. 2002. Optimized treatment planning for prostate cancer comparing IMPT, VHEET and 15 MV IMXT. Physics in Medicine and Biology 47:2247-2261.